# Mechanical properties of a two-filament bundle

Author: Laura Roman Canal

*Facultat de Física, Universitat de Barcelona, Diagonal 645, 08028 Barcelona, Spain.*[*]

Advisor: M. del Carmen Miguel López

**Abstract:** In this work we study the interplay between elastic degrees of freedom and crosslink binding dynamics of a two filament bundle slowly driven into a bent state. Using Monte Carlo simulations, we will measure the crosslinks density as a function of crosslink stiffness and for given bending amplitudes. The results show that only hard crosslinks present collective unbinding at a certain bending amplitude, leading to a first order phase transition between unbound-bound states.

## I. INTRODUCTION

Over the past decade, the study of polymers has raised a great interest in the field of soft condensed matter due to the key role bundles of filamentous polymers play in biological processes, p.e. conforming extracellular and intracellular structures. One example is the *cytoskeleton* (Fig. 1), which ensures the cell's structural integrity and mobility and also regulates intracellular organization and transport [1]. Thanks to the accessibility to cellular environments, many experimental studies have been performed on biopolymers. The results obtained, sometimes striking different to the behavior of synthetic and flexible polymers, have motivated the theoretical study and characterization of these so called *semiflexible* polymers.

A *semiflexible* polymer is a filament with a bending stiffness (resistance against bending deformation) large enough for its bending energy term to compensate the entropic contribution - that comes from the significant thermal fluctuations of the system- so the straight conformation dominates over the tendency of the filament to adopt a *random coil* conformation, [2]. This competition between energetic and entropic effects gives rise to behaviors unique of semiflexible polymers, mainly due to their dimensions and mechanical properties, p.e. its bending stiffness. To characterize the bending stiffness of a polymer we introduce the *persistence length* or length over which the polymer appears straight in the presence of Brownian forces, i.e. thermal fluctuations. Experimental studies show that most synthetic polymers have a persistence length much smaller than the polymer relevant length scale, so entropic term dominates over energetic contributions thus leading to the *random coil* conformation. Biopolymers however, tend to be composed of large globular proteins that make the polymer more rigid, so its persistence length is much larger than the molecular scale while it is comparable to the relevant length scale. So we say biopolymers are semiflexible and present a competition between entropic and energetic effects, with the elastic strain energy stored in both stretching and bending deformation modes of filaments, [2, 3].

———————

[*]Electronic address: `lauraromancanal@gmail.com`

Just like the composition of a polymer defines its persistence length and therefore its mechanical behaviour, it also dictaminates the interactions with other polymers. Semi-flexible polymers show difficulty in entanglement - since they cannot readily form knots- and so they are more sensible to form crosslinked bundles. Moreover, the properties of physiological crosslinkers, p.e nonlinear elastic response and dynamic/transient nature, can modify the viscoelastic properties of the bundle. In-vitro experiments and modeling have showed that crosslink stiffness mediates bundle mechanical properties and conversely, bundle conformational changes or the application of a destabilizing forces change the binding state of the crosslinks. On another note, motor proteins such as *myosin* -which can actively generate stochastic forces by pulling on F-actin filaments- can drive the filamentous bundle into a *non equilibrium* state and therefore highly modify the mechanics and dynamics of the system, [2].

The motivation of this work is to study the competition between energetic and entropic effects in a simulated biopolymer bundle at equilibrium. As explained above, these polymers are weakly bound together by reversible crosslinks but exhibit stability and strength in terms of a bending rigidity that competes with thermal bending or stretching fluctuations. In particular, we are interested in understanding the interplay between reversible crosslink binding and bundle mechanical properties when deforming our semi-flexible bundle.

## II. THE MODEL

In this model we consider a two-filament bundle of length $L$ lying in a two-dimensional plane, [4]. These semi-flexible filaments of bending stiffness $k_f$ are spaced a distance $b$ apart and are laterally interconnected by reversible crosslinks, with crosslink shear stiffness $k_x$, that can bind and unbind the filament pair. We characterize each of the filaments as a chain of $j = 1, ..., N_x$ beads (crosslink binding sites) with harmonic springs, of spring constant $k_s$, that laterally join nearest neighboring beads and that are spaced in equilibrium at regular intervals a distance $a$ apart. We will only allow the beads to move along the contour (bundle shape), neglecting the possibility of making any displace perpendicular
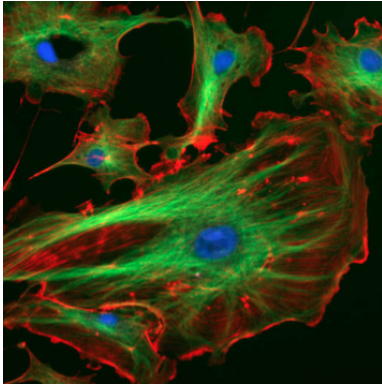
FIG. 1: Fluorescence microscopy image of an eukaryotic cell cytoskeleton: actin filaments (red), microtubules (green), [2].
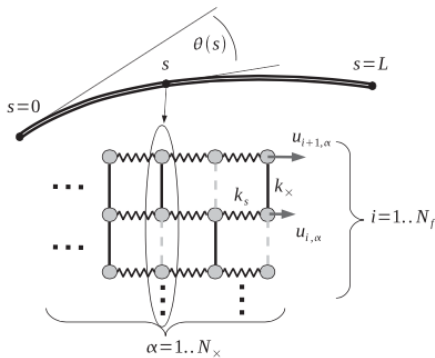


FIG. 2: Representation of the bent state of the bundle characterized by the tangent angle $\theta(s)$ at each $s$ site, [5].

to the bundle axis, thereby reducing the bead movement to be one-dimensional. The bundle is driven into a bent state characterized by the tangent angle $\theta(s)$ at arclength position $s = 0, ..., L$ along the bundle contour (see Fig. 2). We characterize our bundle of $i = 1, ..., N_i$ filaments and $N_x$ beads per filament as a $N_i \times N_x$ dimensional array, where a $(i, j)$ matrix's site is the $j$th-bead on the $i$th-filament, characterized by a lateral displacement $u_{ij}$, an imposed bending angle $\theta_j$ and a crosslink occupation number $n_{ij} = \{0, 1\}$: $n_{ij} = 1$ means a crosslink exists between beads $(i, j)$ and $(i + 1, j)$ and $n_{ij} = 0$ means nonexistence. We will consider the driving to the bent state slow enough so the crosslink binding degrees of freedom can equilibrate at such amplitude, i.e.bundle shape is assumed constant in time. As we implement a deformation-controlled virtual experiment the filaments bending energy is constant and therefore irrelevant in our simulations, in contrast with the worm-like chain (WLC) model proposed by Kratky and Porod, for inextensible biopolymers with finite resistance to bending, [2]:

$$H_b = k_f \sum_{i=1}^{N_f} \sum_{j=1}^{N_x} \left( \theta'_{i,j} \right)^2 \sim ct. \qquad (1)$$

There are two contributions to the elastic energy of the bundle that can not be neglected. One is the stretching energy of the filaments $H_s$, due to the relative displacement of consecutive beads $j$ and $j + 1$ along the $i$th-filament: $(u_{i,j+1} - u_{i,j})$. This energy is characterized by the filament stretching stiffness $k_s$ related to the Young modulus $E$ by $k_s \sim Eb^2/a$. From elemental knowledge of continuum elasticity, we consider the discretized version of the stretching energy term:

$$H_s = \frac{k_s}{2} \sum_{i=1}^{N_f} \sum_{j=2}^{N_x} (u_{i,j-1} - u_{i,j})^2. \qquad (2)$$

As a consequence of bringing the bundle into a bent sate, filaments slip relative to each other and the anchoring of crosslinks with filaments abandons its original perpendicularity. The cost associated to this non-perpendicular anchoring can only be compensated if one of the filaments stretches out farther than the other and compensates the $b\theta$ bending mismatch, i.e. crosslink shear deformation between $(i+1, j)$ and $(i, j)$ beads, $(u_{i+1,j} - u_{i,j} + b\theta_j)$ takes place. Moreover, the possibility of the $(i, j)$ crosslink to unbind $(n_{i,j} = 0)$ must be included in the crosslink shearing energy term, as once it unbinds it decouples its associated beads and reduces to zero its associated shearing energy. The shear contribution to the elastic energy of the bundle is characterized by the crosslink shear stiffness $k_x$, related to the shear modulus $\mu$ by $k_x \sim \mu a$.

$$H_x = \frac{k_x}{2} \sum_{i=1}^{N_f-1} \sum_{j=1}^{N_x} n_{i,j} \left( u_{i+1,j} - u_{i,j} + b\theta_j \right)^2. \qquad (3)$$

The expression for the local tangent angle of the bundle at the $j$ crosslink site comes from the much studied case of and end-grafted bundle deformed by a tip-load at its free end:

$$\theta_j = aCN_x \sin(\pi j/2N_x). \qquad (4)$$

To sum up, in this model the crosslinks can remain unsheared only if filaments stretch out or, on the contrary, filaments can avoid to stretch only at expenses of crosslink shearing. Because the crosslinks can bind and unbind, this translates in saying that the number of crosslinks present in the bundle (those that are bound, $n_{ij}=1$) fluctuates and is determined by:

$$N = \sum_{i=1}^{N_f} \sum_{j=1}^{N_x} n_{i,j}. \qquad (5)$$

So in this model where $N$ is not constant, we are forced to use the grand canonical ensemble. We must take into account a crosslink chemical potential $\mu$ so a binding enthalpy $-\mu N$ is introduced to the bundle model Hamiltonian, that is now defined by:

$$H = H_x + H_s - \mu N. \qquad (6)$$

We therefore consider that the bundle is more stable the more crosslinks are bound.

## A. Setting of parameters

The variables of our model are the number of filaments $N_f$, the number of beads (or crosslink sites) $N_x$, the filament stretching stiffness $k_s$, the crosslink shear stiffness $k_x$, the lattice's constants: bead to bead distance $a$ and filament to filament distance $b$, the bending amplitude $C$, and the crosslink chemical potential $\mu$. Our simulated bundle consists of $N_i = 2$ filaments and $N_x = 100$ beads. We also set the lattice's constants to $a, b = 1$ so the bundle length is defined by $L = aN_x$ is set to $L = 100$ and we introduce an end-grafted bundle condition $u_{i,1} = 0$. The temperature may play an important role in our model and we will set $\beta = 1/k_bT$ to $\beta = 100$ and also $\beta k_s = 100$. We will measure the crosslink density $n = N/N_{max}$ in terms of varying $\mu$, $C$ and the non-dimensional parameter $k_x/k_s$. Here $N_{max}$ is the maximum number of crosslinks that can be bound in our bundle, defined by $N_{max} = N_x(N_f - 1)$. So in our model it is $N_{max} = 100$.

## III. THE METHOD

In order to perform our simulations we write a Monte Carlo FORTRAN program in the Grand Canonical Ensemble, as the $N$ number of crosslinks is a fluctuating quantity. We proceed to give a few hints on how the program was written to understand the method followed. The system is represented by a $(i = 1, ..., N_i) \times (j = 1, ..., N_x)$ lattice. Each $(i, j)$ lattice site has a $u_{i,j}$ relative displacement and a $n_{i,j}$ occupation variable associated, so we must construct two matrices; one per variable. As the binding of a crosslink involves pairs of mirroring beads, the occupation matrix is one dimension smaller than the displacement matrix. So for our two-filament bundle, of $N_x = 100$ beads per filament, there is one single row of paired beads and the occupation of crosslinks is a vector: $OCUP[j], (j = 1, ..., 100)$ while the relative displacements matrix is: $U[i, j], (i = 1, 2; j = 1, ..., 100)$. Once setting initial conditions and defined values and parameters of the model, a typical Monte Carlo routine starts, [6]. However, this MC routine we have written has two singularities: it works in the grand canonical ensemble and at each Monte Carlo step both a displacement move and a crosslink bind/unbind move is attempted. The relative displacement proposed for the randomly selected $i, j$-bead is $u'_{i,j} = u_{i,j} + \delta$, with $-0.1 < \delta < 0.1$ drawn uniformly randomly . The (un)-bind move is spin flip like, i.e. if the randomly selected $j$-bead pair (or lattice site) is occupied by a crosslink it is proposed to be unoccupied, (if $n_{ij} = 1 \rightarrow n'_{ij} = 0$) and vice versa. The acceptance of each movement follows MC acceptance laws but using the Grand-Canonical Hamiltonian, Eq. (6).

At every MC-step the $N$ number of crosslinks is obtained by Eq. (5) so at the end of the MC loop we average $N$ over all $2 \cdot 10^7$ MC-steps and obtain the average

crosslink density defined by:

$$\langle n \rangle = \frac{\langle N \rangle}{N_{max}}. \tag{7}$$

In order to observe the interplay between reversible crosslink binding and bundle mechanical properties for a given $k_x/k_s = 10^{-5}, ..., 10^{-2}$, our program will explore different bending amplitudes $C = 0, ..., 0.4$ and crosslink potentials $\beta\mu = -3, ..., 4$ for $C = 0$

## IV. RESULTS

We now proceed to calculate the average crosslink density $\langle n \rangle$ as a function of the control parameters. Since our aim is to understand the relation between bundle elasticity and crosslink (un)binding dynamics we will perform Monte Carlo simulations, following the method described above, with posterior theoretical analysis.

We are primarily interested in studying two situations. Firstly, we will consider the crosslink occupation density as a function of the crosslink potential $\mu$ for an undeformed bundle. Lastly, we will discuss the crosslink occupation as a function of bundle deformation at a given crosslink potential.

## A. Crosslink occupation as a function of binding energy

We study the dependance of the crosslink occupation density $\langle n \rangle$ with the crosslink potential $\mu$ that characterizes the binding energy $(-\mu N)$ for an undeformed bundle $(c = 0)$ previously characterized. In this situation, there is a competition between the crosslink binding energy and the energetic terms of filament stretching, Eq. (2), and crosslink shearing, Eq. (3). However, for this straight initial configuration of the bundle, the shearing energetic term comes merely from the fluctuations in the relative displacement of beads because $b\theta_j = 0$ as there is no global bending. Figure 3 displays the data obtained in the MC simulations for different crosslink stiffness $k_x/k_s$, where we see the binding of crosslinks in the bundle as a continuous process with no phase transition from the unbound to the bound state. Two main features are observed: crosslink occupation increases with the chemical potential value $(\mu \nearrow)$ and with decreasing crosslink stiffness $(k_x/k_s \searrow)$. These results are in agreement with what we expected for our system described by the hamiltonian at Eq. (5): the $(-\mu N)$ term indicates a favorable situation to have crosslinks bound for $\mu > 0$, and the crosslink shear energetic term, Eq. (3), indicates the greatest the crosslink stiffness is, the more energetically expensive it is to maintain crosslinks bound. We study in detail the crosslink occupation at $\beta\mu = 0$. In this situation there is no longer the energetic term that benefits crosslinks to be bound (binding enthalpy is null) and the equilibrium density occupation is achieved by minimizing

Helmholtz free energy. In soft systems ($k_x/k_s = 10^{-2}$) the entropy dominates its behavior over the elastic energy, and indeed we observe exactly half the number of crosslinks in each one of the two possible states.

An analytical approach to this simulation would be to compare these results with the crosslink occupation density expression for a two-filament non-deformed bundle with only one site ($N = n_1$). The generalized hamiltonian, Eq. (5), is then reduced to a three degrees of freedom one: two relative displacement variables $u_1, u_2$ and the $n$ occupation variable of the single crosslink.

$$H_1(u_1, u_2, n) = \frac{k_s}{2}\left(u_1^2 + u_2^2\right)^2 + \frac{k_x n}{2}\left(u_1 - u_2\right)^2 - \mu n. \tag{8}$$

We can now obtain the analytical expression for the crosslink occupation density using grand canonical ensemble basic knowledge:

$$\langle n \rangle = \frac{1}{\beta Z}\frac{\partial Z}{\partial \mu}, \tag{9}$$

being the grand-canonical partition function:

$$Z = \sum_{n=0}^{1}\int\int \exp(-\beta H_1(u_1, u_2, n))du_1 du_2. \tag{10}$$

Applying Eq. (8) to Eq. (10) and to Eq. (9) we get:

$$\langle n \rangle = \left(1 + e^{-\beta\mu}\sqrt{1 + \frac{2k_x}{k_s}}\right)^{-1}. \tag{11}$$

The solutions of this one-crosslink model are shown with the Monte Carlo results in Fig. 3. Both analytical expression (Eq. 11) and simulations data for $\langle n \rangle$ agree in stating that the increase in crosslink occupation is driven by the interplay between the configurational entropy stored in axial displacements and the crosslink binding energy characterized by $\mu$.

### B. Crosslink occupation as a function of bundle deformation

Let us now discuss the dependance of crosslink occupation density $\langle n \rangle$ with bundle deformation characterized by the angle described in Eq. (4), and associated to a clamped bundle loaded at its free end. We will characterize the bundle deformation with the amplitude of the imposed deformation ($c$) as in the limit of small deformations we obtain $c$ from the bundle curvature by $c \sim \theta'$. In this study we will not consider crosslink binding energy so we set crosslink potential $\mu = 0$.

In Fig. 4 we plot the average crosslink density $\langle n \rangle$ as function of the imposed bending amplitude $c$ for different values of $k_x/k_s$. In all cases, $\langle n \rangle$ decreases with $c$ denoting that crosslinks unbind upon bending, the greater the imposed bundle deformation, the lesser crosslinks remain bound. The reason is that bundle deformation tends to
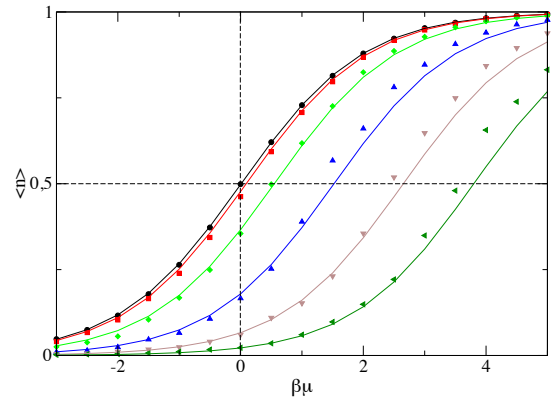


FIG. 3: Average crosslink occupation density as function of control parameter $\beta\mu$ and for $k_x/k_s = 10^{-2}, ..., 10^3$ (from left to right) for a non-deformed two-filament bundle with $\beta k_s = 100$. The solid lines are the solutions of the single crosslink model, Eq. (11).

produce a mismatch between the crosslink binding sites, and therefore an elastic energy cost for the binding as introduced at Eq. (3). However, the striking feature in Fig. 4 is the fact that for a crosslink stiffness high enough ($k_x/k_s = 10^{-2}$) the crosslink occupation density drops extremely sharply at a determined value of bending amplitude $c^*$ so it abandons the smooth and gradual decrease that $\langle n \rangle$ presents for lower values of $k_x/k_s$.

In Fig. (5) we plot the average energy of the bundle as function of the imposed bending amplitude $c$ for the different values of $k_x/k_s$. We can observe that there is a peak in the bundle energy of $k_x/k_s = 10^{-2}$ at $c = c^*$, indicating that there is a characteristic energy barrier associated to the discontinuous drop of crosslink occupation density, i.e. it is a first-order transition from the bound to unbound state. This surprising mechanism cannot be obtained with the one-crosslink model, which describes a smooth decreasing occupation upon bundle deformation governed by a renormalized potential that includes bundle curvature, [5]. In fact, the existence of a discontinuous transition is due to a cooperative effect where many crosslinks must be unbound to drive the bundle into a weakly crosslinked state. Thus, soft crosslinks unbind progressively leading to a smooth decrease of average crosslink occupation upon bending while stiff crosslinks tend to unbind cooperatively with a discontinuous transition. A theoretical approach to this phenomena should be made in the mean-field approximation but it can also be understood in terms of a competition between filament stretch $k_s$ and crosslink shear $k_x$ energy scales, relevant only for stiff crosslinks.

Soft crosslinks ($k_x \searrow$) can not induce a stretching in the filaments when deformed, so the force over the crosslinks is governed by $k_x$ and it is small. Therefore
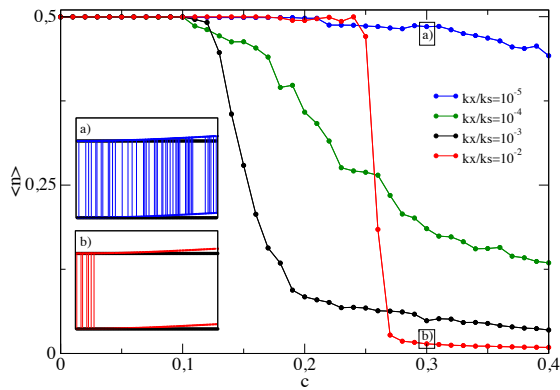
FIG. 4: Average crosslink density as function of bundle deformation $c$ for different crosslink stiffness $k_x/k_s = 10^{-5}, ..., 10^{-2}$. For the largest crosslink stiffness ($k_x/k_s = 10^{-2}$) the simulations display a discontinous drop at $c^*$.



FIG. 5: Average bundle energy as function of bundle deformation $c$ for crosslink stiffness $k_x/k_s = 10^{-5}, ..., 10^{-2}$. The energy peak at $c^*$ for $k_x/k_s = 10^{-2}$ indicates the presence of a free-energy barrier and the first-order nature of the transition.

unbinding events are purely local and do not affect the rest of the bundle, and the decrease of crosslink occupation upon bending is smooth. On the other hand, stiff crosslinks ($k_x \nearrow$) induce stretching in filaments as a result of shearing-stretching competition. Thus, the force over crosslinks is governed by $k_s$ and a crosslink unbinding event modifies the force balance in the filaments. In this limit, the force over crosslinks leads to collective unbinding behavior potentially driving the whole bundle into the unbound state, i.e. at a certain bending amplitude an unbundling first-order phase transition takes place.

## V. CONCLUSIONS

- First of all, we have seen that for an undeformed two-filaments bundle the crosslink occupation is controlled by the interplay between binding energy and the configurational entropy stored in the axial displacement modes, increasing with the crosslink potential with no sudden transition.

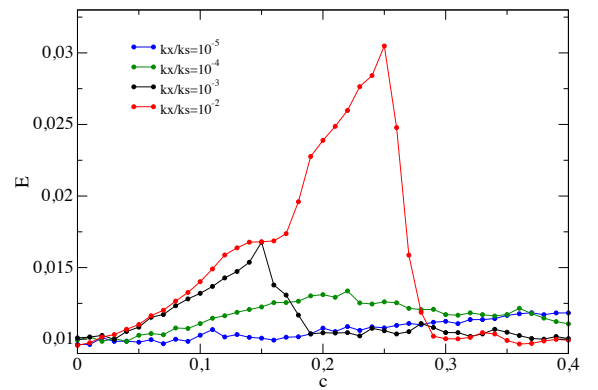- Secondly, we've realized that a two-filament

non-deformed bundle with a single crosslink model can be solved analytically and its solutions for the crosslink occupation reproduce the simulated curves, the smaller the crosslink stiffness, the greater the accuracy.

- Finally, we have studied the response of a reversibly crosslinked two-filament bundle for an imposed bundle deformation. We have concluded that bundle deformation leads to a mismatch between binding sites and therefore to an elastic energy cost for binding that for stiff crosslinks leads to a collective unbind phenomena at a given bundle deformation amplitude, i.e. a first-order phase transition between bind-unbind states.

[1] Alberts, B. et al. "Molecular Biology of the Cell". Garland Press. (1994)
[2] Broedersz, C.P. & MacKintosh, F.C.. "Modeling semiflexible polymer networks". Rev. Mod. Phys. **86**, 995 (2014)
[3] Hatami-Marbini, H. & Picu, R.C.. "Heterogeneous long-range correlated deformation of semiflexible random fiber networks". Physical Rev. E **80**, 046703 (2009)
[4] Vink, Richard L.C. & Heussinger, C.. "Crosslinked biopolymer bundles: crosslink reversibility leads to cooperative binding/unbinding phenomena". J. Chem. Phys. **136**, 035102 (2012)
[5] Heussinger, C.. "Cooperative crosslink (un)binding in slowly driven bundles of semiflexible filaments". Phys. Rev. E. **83**, 050902 (2011)
[6] Frenkel, D. & Smit, B.."Understanding molecular simulation. From algorithms to applications". A. press,(2001)